Crystal structure of a *c-kit* promoter quadruplex reveals the structural role of metal ions and water molecules in maintaining loop conformation

Dengguo Wei, Gary N. Parkinson, Anthony P. Reszka and Stephen Neidle*

CRUK Biomolecular Structure Group, UCL School of Pharmacy, University College London, 29-39 Brunswick Square, WC1N 1AX, London, UK

ABSTRACT

We report here the 1.62 Å crystal structure of an intramolecular quadruplex DNA formed from a sequence in the promoter region of the *c-kit* gene. This is the first reported crystal structure of a promoter quadruplex and the first observation of localized magnesium ions in a quadruplex structure. The structure reveals that potassium and magnesium ions have an unexpected yet significant structural role in stabilizing particular quadruplex loops and grooves that is distinct from but in addition to the role of potassium ions in the ion channel at the centre of all quadruplex structures. The analysis also shows how ions cluster together with structured water molecules to stabilize the quadruplex arrangement. This particular quadruplex has been previously studied by NMR methods, and the present X-ray structure is in accord with the earlier topology assignment. However, as well as the observations of potassium and magnesium ions, the crystal structure has revealed a highly significant difference in the dimensions of the large cleft in the structure, which is a plausible target for small molecules. This difference can be understood by the stabilizing role of structured water networks.

INTRODUCTION

Quadruplex nucleic acids are higher-order structures containing tracts of short guanine-repeats (G-tracts). These structures are formed from one, two or four strands by the self-association of these guanines (1–3), which are involved in stable hydrogen-bonded arrangements (G-quartets). These have two or more G-quartets stacking on one another to form the core platform in all quadruplex structures. The core G-quartets in turn are held together by the intervening sequences; for example the most common intramolecular type of quadruplex is formed by a sequence of type

$$G_aX_nG_bX_oG_cX_pG_d$$

where G_{a-d} represent the G-tracts and $X_{n,o,p}$ are intervening sequences, which form defined loop arrangements. Such quadruplex sequences are found, for example, in telomeric DNA and RNA (4), as well as in a large number of genomic sites (5,6) especially promoter (7–9) and 5′-untranslated RNA sequences (10–12).

Alkali metal ions ($K^+ > Na^+ > Li^+$) are well-established to play a crucial role in the stabilization of G-quadruplexes (13–26), whereas Mg^{2+} ions, by contrast with duplex nucleic acids, has been reported not to do so (27). A recent report though, provides evidence that whereas telomeric quadruplexes are destabilized by Mg^{2+} ions, promoter quadruplexes are stabilized by them (28). NMR (17,20–24) and extensive crystallographic data (29–34) has shown that the O6 oxygen guanine substituents in a G-quartet coordinate the metal ions so that they occupy the centre of a channel formed by successive G-quartets, in a linear or quasi-linear assay. The nature of the coordination is dependent on ionic radius. Thus K^+ ions have exclusively bi-pyramidal anti-prismatic arrangements that involve the ion being at the centre of two successive G-quartets. Smaller Na^+ ions, by contrast, are able to be coordinated in a square planar arrangement within a single G-quartet, although in practice Na^+ ions are found at varying positions relative to G-quartet planes. Recent K^+ titration experiments have suggested that for human telomeric quadruplexes, folding requires more than the number of K^+ ions required for the channel alone (35).

The presence of the alkali metal ions is essential for the folding of a quadruplex, and the nature of the ion involved can profoundly alter the particular topology that is formed. This has been extensively explored in particular for intramolecular telomeric quadruplexes, but is not

---

*To whom correspondence should be addressed. Tel: +44 207 753 5969; Fax: +44 207 753 5970; Email: s.neidle@ucl.ac.uk

explicable by any minor changes in the ion channel on exchanging, for example, K^+ to Na^+. The 22-mer four-repeat human intramolecular telomeric quadruplex forms a well-defined anti-parallel quadruplex in Na^+ solution (36) as revealed by NMR studies, having one lateral and two diagonal loops. By contrast a variety of forms have been observed for K^+-containing four-repeat human intramolecular telomeric quadruplex sequences, sometimes with propeller and lateral loops or as in the case of that found in a crystal structure, all-propeller loops and parallel topology (37–41). The precise mechanistic role of metal ions in producing these transitions, or indeed in overall quadruplex stabilization, has not been apparent. It has long been known though that stabilization does require a higher concentration of ions than would be required solely for formation of an ion channel. Except for supporting the G-quartets in the channel of quadruplex, are there any other roles that ions are able to play in inducing folding or stabilizing the final structure?

We have approached this problem by focusing on an intra-molecular quadruplex (*c-kit1*) from the *c-kit* promoter, which has been previously characterized by NMR methods (42,43), initially in order to ascertain the extent to which crystal and NMR structures would agree, and as a prelude to more detailed structure-based ligand design studies. The *c-kit* gene and its protein product play an important role in several human malignancies, notably gastro-intestinal (GIST) tumours and there has been considerable interest in down-regulating *c-kit* expression by directly intervening at the promoter level, by stabilizing one or other of the quadruplexes encoded in the *c-kit* promoter with small molecules (44,45). The *c-kit*1 quadruplex sequence has a unique occurrence in the human genome and modelling studies have suggested that the structure itself may also be unique (46). The crystal-structure analysis presented here has confirmed the overall topological features as found by NMR, although there are a number of significant structural differences in those regions of the quadruplex that could be of especial importance for ligand binding. In addition the resolution of this structure, combined with the exceptional quality of the diffraction data, have revealed a number of novel and unexpected features about the structural role of metal ions, which have relevance to the stability of quadruplexes in general.

MATERIALS AND METHODS

Crystallization and data collection

A brominated uridine residue was incorporated into the *c-kit*1 quadruplex sequence d($AG_3AG_3CGC[^{Br}U]G_3AGG$ AG_3), which was synthesized and purified as described previously (29), in order to aid crystallographic phasing. This sequence is identical to that used for the NMR studies, apart from the ^{Br}U residue replacing a thymine. A 2 mM DNA solution was used, containing 20 mM potassium cacodylate buffer at pH 6.5 and 50 mM potassium chloride and heated to 358 K before annealing by slow cooling to room temperature. Crystals were grown by the hanging drop vapour diffusion method. An amount of 1 µl of a premixed drop solution containing 10% MPD, 10 mM magnesium chloride, 50 mM potassium chloride, and 50 mM sodium cacodylate at pH 6.5, was added to 1 µl of *c-kit*1 DNA solution at a concentration of 2 mM. The drop solution was equilibrated against a 50% MPD well solution at 283 K. A few crystals appeared after 2 months but required a seeding protocol in order to obtain reproducible crystals. These had large thin flat plate morphology. Two datasets were collected at 105 K on two single flash-frozen crystals at the Diamond synchrotron facility. SAD data was collected at a wavelength of 0.9198 Å (the theoretical SAD wavelength of bromine), and a native dataset was collected at a wavelength of 0.9763 Å.

Structure solution and refinement

The positions of two bromine atoms were determined by Patterson methods. Phases were subsequently calculated by the SHELX-C/D/E program (47), using the SAD dataset. Two further peaks, with a ~3.5 Å separation, were tentatively identified as a pair of channel potassium ions in one quadruplex structure. Some of the stacked G-quartets could be recognized at this stage. The G-quartets extracted from the human telomeric quadruplex crystal structure (PDB code 1K8P) were modified to obtain an initial model for electron-density fitting. Molecular Replacement utilized the revised quadruplex model was sufficient to determine the relative configuration of the two quadruplex structures completing one asymmetric unit. Other parts of the quadruplex structures were progressively built on the basis of the $2F_o$–F_c and F_o–F_c difference electron density maps derived from the 20–2.8 Å diffraction data. This was followed by the location of the majority of the water molecules. Finally, the 1.62-Å data set collected at the native wavelength (0.9763 Å) was used for high-resolution refinement, and the other K^+ ions and Mg^{2+} ions were unequivocally assigned by considerations of coordination numbers and coordination distances. After further refinement the complete water network could be seen clearly. A total of 212 water molecules are included in the final structure. Final R and R_{free} values are 0.166 and 0.213, respectively. Coordinates and structure factors are available from the PDB as entry 3QXR. Diffraction data were processed by the SCALE program in the CCP4 package (48), and COOT (49), PHASER (50) and REFMAC5 (51) were used in the processes of model fit, building and refinement. Programs CHIMERA (52) and PYMOL (53) (http://www.pymol.org) were used for visualization and analysis. Table 1 details crystallographic data.

A movie showing the details of the crystal structure can be downloaded from http://www.bmsg.ulsop.ac.uk/people/DengguoWei.html.

RESULTS

Overall features of the structure

The *c-kit*1 crystals reported here are in space group $P2_12_12$, and have two independent quadruplexes in the

Table 1. Crystallographic data collection and refinement statistics

Sequence	d(AGGGAGGGCGC[^{Br}U]GGGAGGAGGG)	
Data collection		
Space group	$P2_12_12$	
Cell dimensions		
a, b, c (Å)	37.57, 51.35, 58.34	
	Crystal 1[a]	Crystal 2[a]
Wavelength (Å)	0.9198	0.9763
Resolution (Å)	58.23–1.98	38.55–1.62
R_{merge}	0.115 (0.611)	0.057 (0.38)
I/σ	13.4 (3.4)	27.4 (2.4)
Completeness (%)	96.8 (91.7)	93.2 (61.8)
Redundancy	7.8 (7.9)	3.6 (2.6)
Total no. of reflections	62 737 (4236)	50 085 (1741)
No. of unique reflections	8049 (535)	14 007 (669)
Refinement		
Resolution (Å)		26.9–1.62
No. of reflections		13 279
R_{work}/R_{free}		0.176/0.221
No. of ions		11.5
No. of water molecules		210.5
Overall B factor (Å^2)		20.07
RMSD in:		
Bond length (Å)		0.005
Bond angle (°)		1.0
PDB ID		3QXR

[a]For Crystal 1, values in parentheses refer to the highest resolution shell, 2.03–1.98 Å; for Crystal 2, values in parentheses refer to the highest resolution shell, 1.66–1.62 Å.

asymmetric unit (A and B) that are stacked on each other in a head-to-head manner (Figure 1a). Each 22-base DNA sequence folds into a parallel four-stranded G-quadruplex. The isolated non-G-tract guanine (G10) is embedded in the G-quartet core, and there are four loops in the structure (Figure 1b). Two single-residue linkers (A5 and C9) form two propeller (double-chain reversal) loops that bridge three G-quartet layers. C11 and ^{Br}U12 form the third loop, which connects two G-quartet corners (G10 and G13). The stem-loop formed by the five-residue sequence A16–G17–G18–A19–G20 allows the terminal G21–G22 to be inserted back to the G-quartet core. These two quadruplex structures have a high degree of structural conservation, which extends to the five-residue long loop, ions, the structural water molecules and the hydrated water molecules. The main differences between quadruplexes A and B are in the detailed conformations of the residues at the quadruplex dimer stacking interface (A1, C11 and ^{Br}U12) (Figure 2). The cytosine base of C11 adopts two distinct conformations (*syn* and *anti*) in Quadruplex A, and both have been included in the deposited structure, with half-occupancy for each.

A potassium ion bridges between loop residue C11 and G-quartet residue G21 and the related water molecular network

In addition to the expected potassium ions in the central ion channel, the high quality of the electron density in this
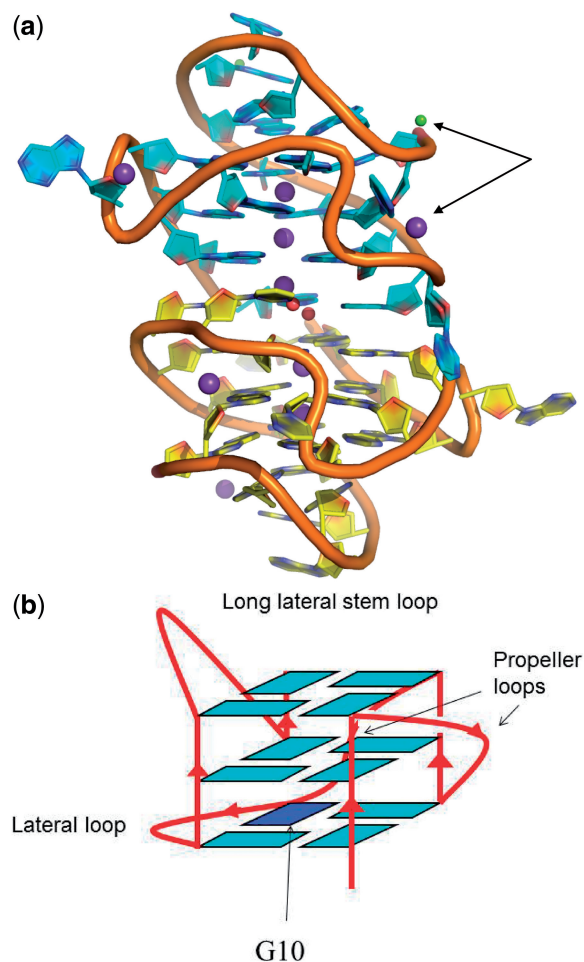

Figure 1. (**a**) Cartoon representation of the two *c-kit*1 independent quadruplexes in the asymmetric unit. Mauve and green spheres represent K$^+$ and Mg^{2+} ions, respectively. Quadruplex A is coloured cyan and B is yellow. The environment of the ions indicated by arrows is detailed in Figure 3a. (**b**) Schematic representation of the topology of the c-kit1 quadruplex.

crystal structure has revealed the existence of potassium ions located in the loops and grooves (Figure 3). Thus, two well-defined non-channel K$^+$ ions are associated with each quadruplex, situated close to the exterior surface but playing key roles in maintaining the structural integrity of particular regions. They are involved in extensive intramolecular contacts, but play no direct role in packing interactions between quadruplexes in the crystal lattice. Thus they may be considered as integral to this quadruplex structure.

One K$^+$ ion in each independent quadruplex is sandwiched in a groove and sits symmetrically between a phosphate oxygen atom of C11 and the O4′ deoxyribose sugar ring atom of G21, with coordination to both oxygen atoms (Figure 3a and b). This K$^+$ ion is octahedrally coordinated, with four water molecules in an approximately square-planar arrangement in addition to the two direct quadruplex contacts, and two of them interact with the phosphate group of ^{Br}U12 in quadruplex A (Figure 3a) and one with ^{Br}U12 in quadruplex B
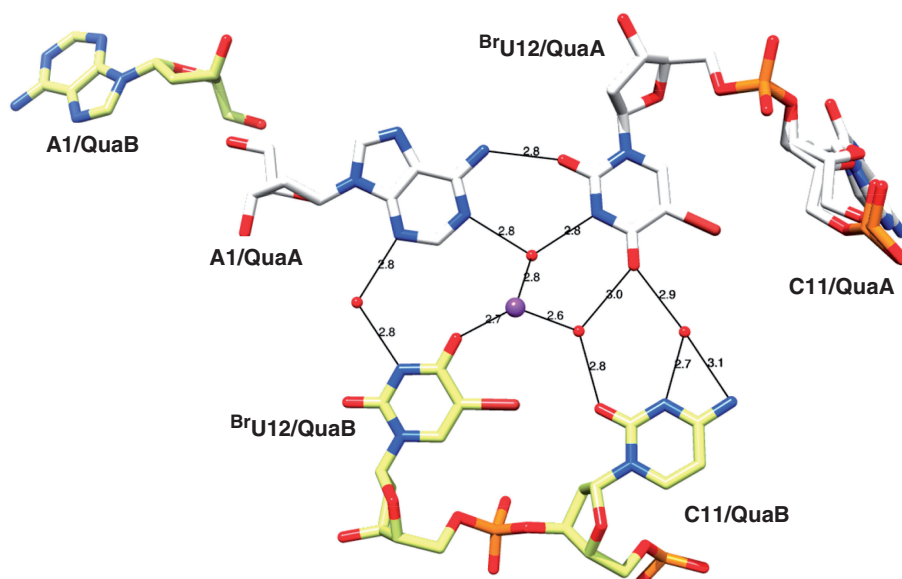
Figure 2. The nucleotides (A1, C11 and ^{Br}U12) at the interface between the two quadruplexes in the crystallographic asymmetric unit, with hydrogen bonds shown as black lines. Carbon atoms in the residues of Quadruplex A are coloured white, and those of Quadruplex B are yellow. The K$^+$ ions are shown as magenta spheres and water molecules are represented by the red spheres.

(Figure 3b). Thus this K$^+$ ion directly plays a role in maintaining the conformation of the C11–^{Br}U12 loop and is in a virtually identical position in the two quadruplexes (Figure 3a and b).

This K$^+$ ion is also at the nucleus of an array of well-ordered water molecules that extends side-wards and upwards. The network forms pentagons and hexagons that fill most the available space around the ion. One especially crucial water molecule (HOH211 in quadruplex A: Figure 3a; HOH45 in quadruplex B: Figure 3b) in this network bridges between the phosphate group of G10, the exocyclic N2 group of G7 and the O4′ atom of G8, thus maintaining the particular conformation of the single-nucleotide loop formed by C9. The K$^+$ ion and its associated water networks also link four G-quartet residues (G7, G8, G10 and G21) to two loops (the C9 propeller loop and the C11/^{Br}U12 lateral loop), contributing to the stability of the overall quadruplex structure. This K$^+$ ion in Quadruplex A together with five water molecules forms a discrete hexagonal array and a two-pentagon array in quadruplex B. In quadruplex A, the most distant of these water molecule (HOH65) from the K$^+$ ion, directly coordinated to a Mg^{2+} ion in an adjacent groove, effectively linking the two metal ions through two spines each of three water molecules (Figure 3a and b).

The second non-channel K$^+$ ion in each quadruplex

The complete shell of water molecules around the second non-channel K$^+$ ion in each quadruplex is visible in the electron-density maps and this ion is in distinct environments in the two quadruplexes (Figure 4a and b). This suggests that whereas the role of the first K$^+$ ion discussed above is an invariant feature of the structure, other K$^+$ ions are more able to adopt several distinct positions. This second K$^+$ ion in Quadruplex A bridges between

the O4′ atom of A5 and a phosphate oxygen atom of G7 (Figure 4a), maintaining the conformation of the A5 single-nucleotide loop. The second K$^+$ ion in Quadruplex B, together with a water molecule, bridges between A16 and G15 in the stem-loop (Figure 4b), forcing the bases to adopt a pronounced tilt.

The potassium ions in the channel

Each quadruplex has two K$^+$ ions in its central ion channel. These two parallel channels do not form a continuous straight line, but are separated by ~1.5 Å. The K$^+$ ions channel are all octahedrally coordinated through the G-quartet edges to guanine O6 atoms, as expected. The interface between the two quadruplexes comprises a A-^{Br}U-^{Br}U-C quartet with 2 nt arising from each quadruplex. This quartet is bounded by a fifth channel K$^+$ ion with low mobility and two adjacent water molecules (Figure 2) which forms direct contacts with O6 atoms of G2, G6, G10 and G13 of Quadruplex A, and coordinates with O4 of ^{Br}U12 in Quadruplex B as well as two other water molecules.

The Mg^{2+} ions in the crystal structure

Two Mg^{2+} ions have been identified in the structure, each associated with the corresponding quadruplex. They are in closely similar environments, and are briefly discussed above in relation to an adjacent K$^+$ ion. Both have direct contact with an oxygen atom of the G21 phosphate group (Figure 3a and b). In Quadruplex A, a single water molecule bridges between the Mg^{2+} ion and the G22 phosphate group (Figure 3a), whereas in Quadruplex B, several water molecules are involved in bridging (Figure 3b). Although it appears that these two Mg^{2+} ions are involved in maintaining structural integrity to the same extent as the K$^+$ ions, they have close electrostatic
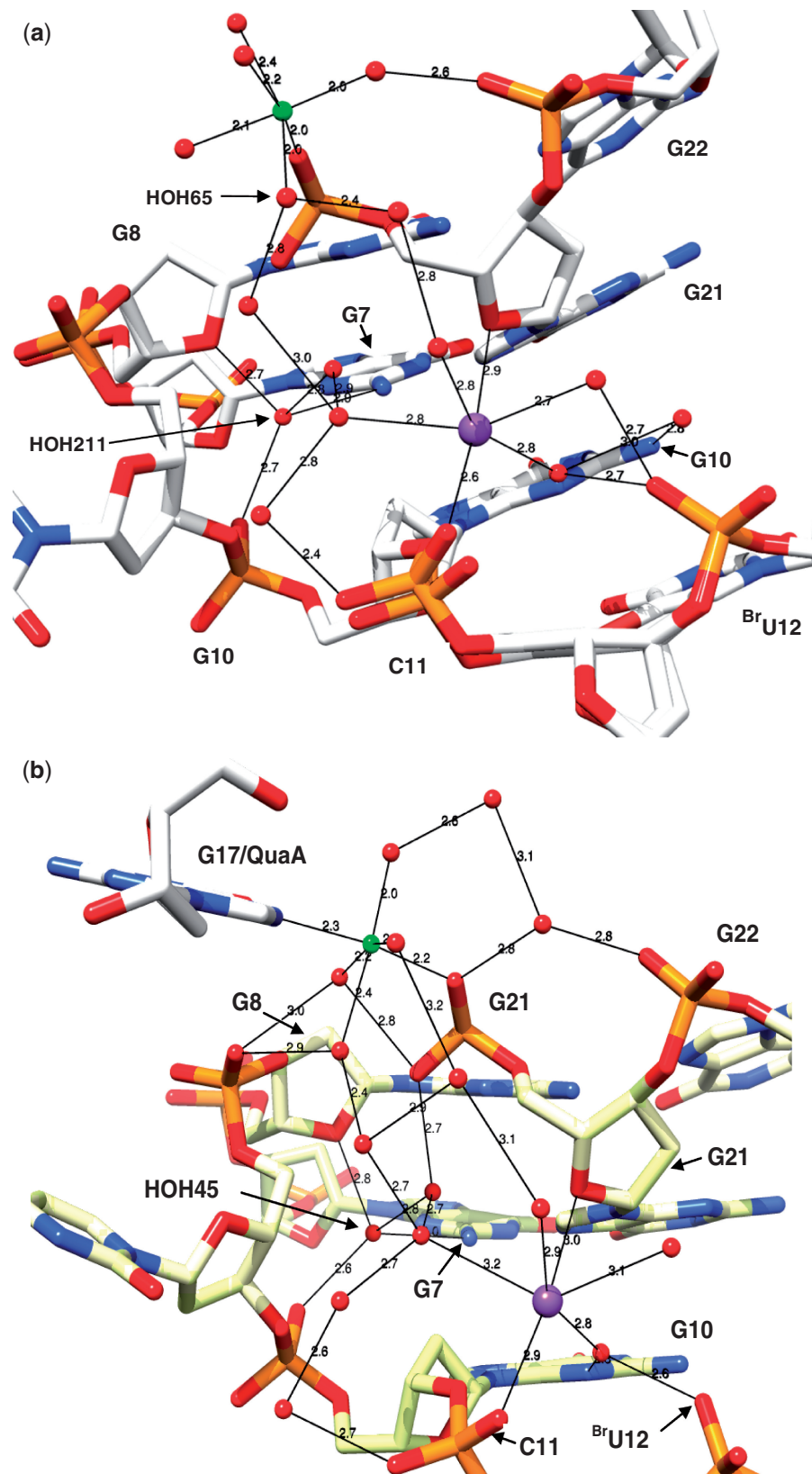
Figure 3. (**a**) Expanded view of the environment of the K$^+$ ion (coloured mauve) in Quadruplex A, with hydrogen bonds shown as black lines. Water molecules are coloured red. The Mg^{2+} ion (in green) is shown connected by a hexagon of water molecules. (**b**) The same view, of Quadruplex B.
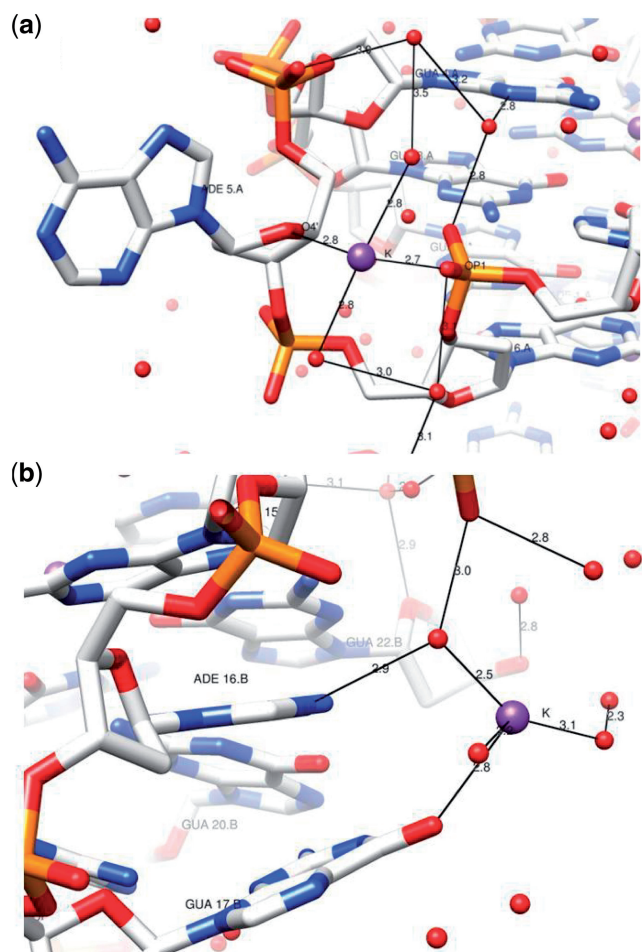
(a)

(b)

Figure 4. The contrasting environment of the second non-channel K^+ ions (**a**) in Quadruplex A, and (**b**) in Quadruplex B. Note that the K^+ ion in the former bridges between a phosphase group and a sugar O4' atoms whereas in Quadruplex B the ion effectively bridges between two adjacent bases.

interactions with phosphate groups, suggesting that their role is secondary, helping to shield the anionic charge of the phosphate groups.

The conserved water molecules in the two crystallographic quadruplexes

The water molecules form extensive extended networks, with a number of waters being highly conserved between the two independent quadruplexes. There are well-ordered spines of hydration in the quadruplex grooves which are not detailed here, but are shown in the movie. Several of the conserved water molecules are responsible for some of the major differences between the NMR and crystal structures (Figure 5a). The most pronounced difference involves the large cleft between the stem-loop and the adjacent G-quartet. This cleft is closed up in the crystal structure, by ~7 Å compared to the NMR models (Figure 5a). This is manifest in a number of conformational differences, which are most pronounced for nucleotides A19 onwards, and are most likely due to the presence of conserved networks

of bridging water molecules, such as are shown in Figure 5b. Here, 3 nt (A16, G17 and A19) are held together across the cleft by hydrogen bonding involving several water molecules that are conserved in the two independent molecules in the crystallographic asymmetric unit, HOH43, 56 and 112. A number of other waters in the grooves are also conserved, although they do not play structural roles to the same extent.

Conformational features

Table 2 details backbone and glycosidic torsion angles in the crystal and NMR structures for the terminal 7 nt. It is notable that differences between the two crystallographic quadruplexes are insignificant for most of the angles, and the largest deviations (32–39°) are for three bonds at the G18/A19 interface. These differences are still not large and do not make a significant difference to the conformations of these two residues. On the other hand there are some large differences in individual torsion angles within the ensemble of NMR models in this general region, affecting residues G18, A19 and G20. These differences are much greater than those involving the crystallographic one, up to 200°, and are mostly indicative of phosphate group flexibility. Table 2 shows that the largest differences between crystal and NMR are also involving the same residues G18, A19 and G20. It is striking that all the torsion angles in the NMR ensemble that indicate the greatest flexibility are among those with the largest differences between NMR and crystal structure torsion angles. The net effect of these differences is that the large cleft is much narrower in the crystal structure, by ~7 Å and A19 is moved in concert with this change (Figure 5a), where it is involved in the hydrogen bonding network detailed above (Figure 5b).

DISCUSSION

This is the first report of any crystal structure for a promoter quadruplex. It is gratifying to note that the structure shows broad correspondence with the NMR structure. This gives added confidence to structure-based design studies and also shows that the dichotomy between crystal (29) and solution structures (37–41) that is apparent for human telomeric quadruplexes (albeit with subtly distinct sequences), is not generally applicable to other eukaryotic quadruplexes.

The high quality of the electron density in this *c-kit*1 crystal structure has enabled both non-channel potassium and magnesium ions to be unequivocally located. The fact that some of these have closely similar positions and co-ordination patterns in both crystallographically independent quadruplexes suggests that these are not artefacts of the crystal lattice but are inherent components of this particular quadruplex and play a role in maintaining its topology and detailed pattern of loop conformations/cleft geometry. The differences between the NMR and crystal structure that are centred around A19 and the cleft are real and indicative of the relative lack of nOe signals in the NMR spectrum for this part of the structure. The fact that a well-defined and conserved water structure
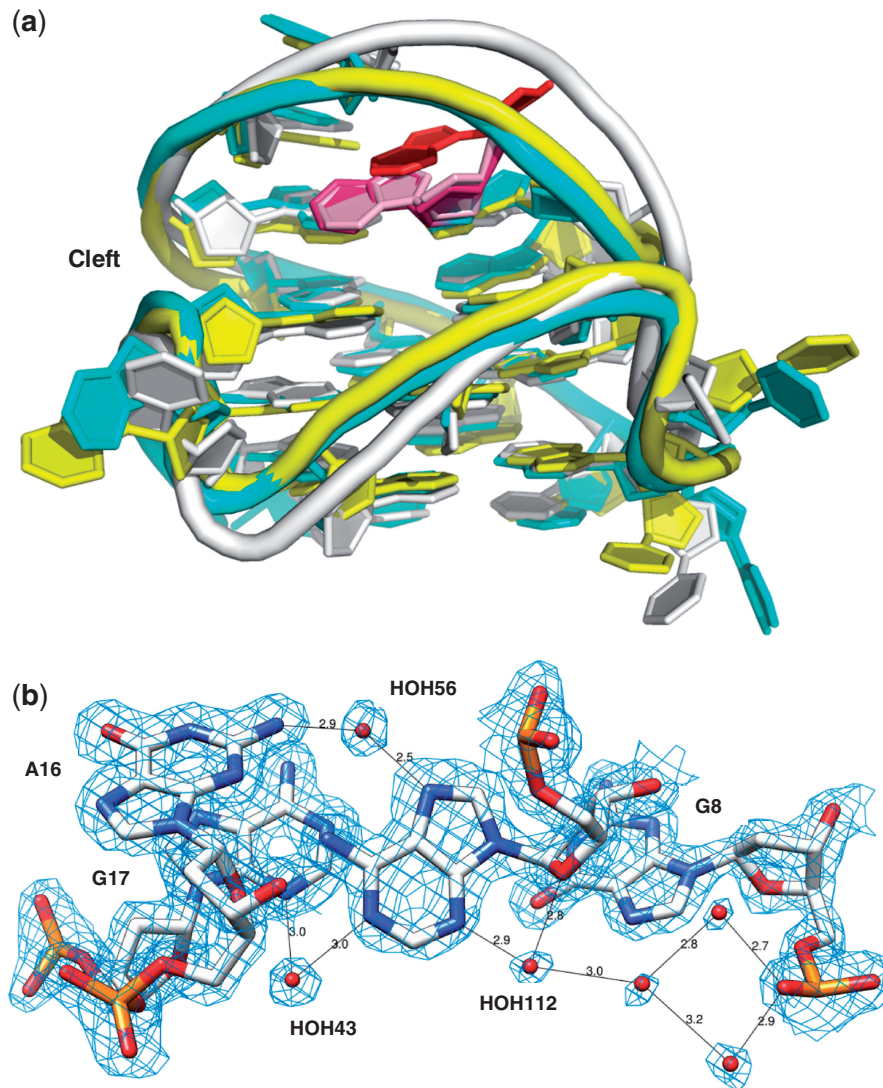
Figure 5. (a) Cartoon representation of the NMR c-kit1 structure (grey) overlaid with the two independent molecules in the crystal structure, Quadruplex A (yellow) and B (cyan). Nucleotide A5 is shown on the left-hand side and the stem-loop is at the top. The A19 adenine base is coloured dark red in the NMR structure and the A19 bases in the crystal structure are coloured mauve. (b) View of the conserved water molecules in the cleft of the crystal structure (shown for Quadruplex A). HOH43, 56 and 112 all interact with and stabilize the conformation of A19. The electron density in the $2F_0 - F_c$ map is also shown. It has been contoured at the 1.0σ level.

has been identified, gives further credence to the crystal structure showing the detail that the NMR analysis is less able to fully represent. The key structural roles of a number of water molecules are reminiscent of the sequence-dependent spine of hydration in B-form duplex DNA (54). The role of water in stabilizing particular structural features of quadruplexes is likely though to be more structure-dependent.

Does the present finding of structured K^+ ions provide insight into the observations of major conformational and topological change found for a number of quadruplexes on changing the nature of the ion [e.g.(36–41)]? The present crystal structure cannot indicate whether the role of the loop potassium ions is in kinetic control (the folding process) or in thermodynamic control (final stabilization). What however is clear is that the structural role for K^+

ions in this structure is dependent on the ionic radius of this ion and its ability to form coordination contacts in the range 2.6–3.2 Å. Na^+ ions, by contrast, typically form coordination contacts that are ~0.3 Å shorter. This would bring the K^+-coordinated nucleotides G10 and G21 almost 0.6 Å closer (Figure 3a and b): whether such a difference would cause large-scale structural changes in the quadruplex remains to be established by further experimental and computational approaches (55–57). Compared with the well-resolved NMR spectrum of the *ckit*-1 quadruplex in K^+ solution (43), the broad and unresolved envelope spectrum of its counterpart in Na^+ solution may signify multiple conformations or aggregation in solution. Soaking *c-kit*1 crystals overnight with a solution containing 200 mM Na^+ did not change the structures or the position of the K^+ ions, indicating (i) that it is

Table 2. List of backbone torsion angles (°) in the two crystallographically independent quadruplexes (QuadA and QuadB) and in the NMR structures

		Crystal		NMR	NMR_torsion angles			Differences			
		QuadA	QuadB	Model 1	Smallest	Largest	$|\Delta_{NMR}|$	$|\Delta_{cryst}|$	|NMR1- QuadA|	|NMR1- QuadB|
A16	α	−58	−69	−79	−89	−78	11	11	21	10
	β	167	169	−174	−176	180	4	2	17	11
	γ	55	58	58	57	62	5	3	3	0
	δ	138	143	134	131	136	4	5	4	5
	ε	−176	−174	−174	−180	−172	7	3	3	0
	ζ	−96	−98	−82	−88	−81	7	2	14	16
	χ	−91	−95	−101	−107	−97	10	4	11	7
G17	α	−62	−73	−63	−65	−59	6	11	1	11
	β	175	168	157	155	161	13	7	18	11
	γ	61	70	69	67	69	2	11	8	2
	δ	157	145	132	131	137	6	12	26	13
	ε	−98	−104	−178	−179	−174	5	6	80	75
	ζ	163	165	−123	−127	−121	7	2	74	72
	χ	−80	−99	−110	−111	−106	5	19	29	10
G18	α	−64	−43	−51	−54	−50	4	21	13	7
	β	134	131	150	147	154	7	3	16	19
	γ	53	34	67	65	68	2	19	13	32
	δ	153	144	123	122	124	2	9	31	21
	ε	−112	−101	−142	−156	−66	90	11	30	41
	ζ	**62**	**101**	**174**	**−169**	**180**	**11**	**39**	**112**	**73**
	χ	−78	−86	−127	−127	−124	3	8	49	41
A19	**α**	**−151**	**177**	**64**	**−38**	**73**	**111**	**32**	**215**	**113**
	β	−139	−177	−132	−134	−90	45	38	8	45
	γ	**56**	**65**	**177**	**−177**	**179**	**4**	**9**	**121**	**112**
	δ	106	94	139	139	141	2	12	32	45
	ε	−98	−101	−159	−161	−140	22	3	62	58
	ζ	**−63**	**−66**	**164**	**−98**	**166**	**96**	**3**	**228**	**230**
	χ	−74	−75	−49	−49	−47	1	1	25	26
G20	**α**	**−88**	**−85**	**97**	**−95**	**100**	**194**	**3**	**185**	**182**
	β	**81**	**83**	**−92**	**−93**	**47**	**140**	**2**	**173**	**175**
	γ	−180	−179	179	165	179	14	1	1	1
	δ	115	124	129	126	144	18	9	14	5
	ε	−152	−148	−116	−117	−116	1	4	36	31
	ζ	−90	−91	−73	−73	−72	1	1	17	19
	χ	−95	−93	−114	−114	−108	6	2	18	21
G21	**α**	**176**	**167**	**−65**	**−68**	**−63**	**5**	**9**	**241**	**233**
	β	178	180	164	161	165	4	2	15	16
	γ	**45**	**46**	**−58**	**−59**	**−57**	**2**	**1**	**103**	**104**
	δ	98	95	130	129	132	3	3	32	35
	ε	−130	−139	−158	−161	−148	13	9	28	19
	ζ	−77	−74	−77	−82	−74	8	3	0	3
	χ	166	170	177	176	177	1	4	11	7
G22	α	−72	−71	−92	−97	−83	14	1	20	21
	β	−166	−162	−147	−156	−142	13	4	18	15
	γ	47	51	50	47	51	3	4	3	2
	δ	152	150	143	141	145	5	2	9	7
	χ	−104	−106	−103	−105	−100	5	2	1	3

Average estimated standard deviations in the crystal structure are likely to be ±1–2°. The NMR deposition in the PDB (PDB id 2KYP) comprises an ensemble of 11 structures. The first NMR structure in the ensemble was taken as a 'representative' example (Model 1: NMR1 in the table). The differences between the smallest and largest individual torsion angles in the 11 NMR structures (Δ_{NMR}) are shown, as well as the differences between the two quadruplexes A and B in the asymmetric unit (Δ_{cryst}) and the differences between NMR and crystal structures. The eight angles that show the greatest differences (>100°) between NMR and crystal structure, are highlighted in bold (defined as |NMR1– QuadA| and |NMR1– QuadB|).

difficult displacing bound K^+ ions in the *ckit*-1 quadruplex crystal structure, and (ii) that this structure is very stable. The role of magnesium ions in stabilizing this particular quadruplex has been previously noted (28), with the finding that the addition of Mg^{2+} did not change topology, as shown by CD spectra, but increased thermodynamic stability, as indicated by the changes in T_m values. This is in accord with the present finding of a discrete structural stabilizing role for Mg^{2+} ions.

ACCESSION NUMBER

3QXR.

REFERENCES

1. Davies,J.T. (2004) G-quartets 40 years later: from 5′-GMP to molecular biology and supramolecular chemistry. *Angew. Chem. Intl. Edit.*, **43**, 668–698.
2. Burge,S., Parkinson,G.N., Hazel,P., Todd,A.K. and Neidle,S. (2006) Quadruplex DNA: sequence, topology and structure. *Nucleic Acids Res.*, **34**, 5402–5415.
3. Phan,A.T., Kuryavyi,V., Luu,K.N. and Patel,D.J. (2007) Structure of two intramolecular G-quadruplexes formed by natural human telomere sequences in K^+ solution. *Nucleic Acids Res.*, **35**, 6517–6525.
4. Phan,A.T. (2010) Human telomeric G-quadruplex: structures of DNA and RNA sequences. *FEBS J.*, **277**, 1107–1117.
5. Todd,A.K., Johnston,M. and Neidle,S. (2005) Highly prevalent putative quadruplex sequence motifs in human DNA. *Nucleic Acids Res.*, **33**, 2901–2907.
6. Huppert,J.L. and Balasubramanian,S. (2005) Prevalence of quadruplexes in the human genome. *Nucleic Acids Res.*, **33**, 2908–2916.
7. Huppert,J.L. and Balasubramanian,S. (2007) G-quadruplexes in promoters throughout the human genome. *Nucleic Acids Res.*, **35**, 406–413.
8. Siddiqui-Jain,A., Grand,C.L., Bearss,D.J. and Hurley,L.H. (2002) Direct evidence for a G-quadruplex in a promoter region and its targeting with a small molecule to repress c-MYC transcription. *Proc. Natl Acad. Sci. USA*, **99**, 11593–11598.
9. Balasubramanian,S., Hurley,L.H. and Neidle,S. (2011) Targeting G-quadruplexes in gene promoters: a novel anticancer strategy? *Nature Rev. Drug Discov.*, **10**, 261–275.
10. Kumari,S., Bugaut,A., Huppert,J.L. and Balasubramanian,S. (2007) An RNA G-quadruplex in the 5' UTR of the NRAS proto-oncogene modulates translation. *Nature Chem. Biol.*, **3**, 218–221.
11. Huppert,J.L., Bugaut,A., Kumari,S. and Balasubramanian,S. (2008) G-quadruplexes: the beginning and end of UTRs. *Nucleic Acids Res.*, **36**, 6260–6268.
12. Halder,K., Wieland,M. and Hartig,J.S. (2009) Predictable suppression of gene expression by 5'-UTR-based RNA quadruplexes. *Nucleic Acids Res.*, **37**, 6811–6817.
13. Howard,F.B. and Miles,H.T. (1982) Poly(inosinic acid) helices: essential chelation of alkali metal ions in the axial channel. *Biochemistry*, **21**, 6736–6745.
14. Hardin,C.C., Henderson,E., Watson,T. and Prosser,J.K. (1991) Monovalent cation induced structural transitions in telomeric DNAs: G-DNA folding intermediates. *Biochemistry*, **30**, 4460–4472.
15. Williamson,J.R., Raghuraman,M.K. and Cech,T.R. (1989) Monovalent cation-induced structure of telomeric DNA: the G-quartet model. *Cell*, **45**, 167–176.
16. Smith,F.W. and Feigon,J. (1992) Quadruplex structure of *Oxytricha* telomeric DNA oligonucleotides. *Nature*, **356**, 164–168.
17. Rovnak,D., Baldus,M., Wu,G., Hud,N.V., Feigon,J. and Griffin,R.G. (2000) Localization of $^{23}Na^+$ in a DNA quadruplex by high-field solid-state NMR. *J. Am. Chem. Soc.*, **122**, 11423–11429.
18. Smirnov,I.V., Kotch,F.W., Pickering,I.J., Davis,J.T. and Shafer,R.H. (2002) Pb EXAFS studies on DNA quadruplexes: identification of metal ion binding site. *Biochemistry*, **41**, 12133–12139.
19. Sen,D. and Gilbert,W. (1990) A sodium-potassium switch in the formation of four-stranded G4-DNA. *Nature*, **344**, 410–414.
20. Schultze,P., Hud,N.V., Smith,F.W. and Feigon,J. (1994) The effect of sodium, potassium and ammonium ions on the conformation of the dimeric quadruplex formed by the *Oxytricha nova* telomere repeat oligonucleotide $d(G_4T_4G_4)$. *Nucleic Acids Res.*, **27**, 3018–3028.
21. Marincola,F.C., Virno,A., Randazzo,A., Mocci,F., Saba,G. and Lai,A. (2009) Competitive binding exchange between alkali metal ions (K^+, Rb^+, and Cs^+) and Na^+ ions bound to the dimeric quadruplex $[d(G_4T_4G_4)]_2$: a ^{23}Na and ^1H NMR study. *Magn. Reson. Chem.*, **47**, 1036–1042.
22. Ida,R., Kwan,I.C. and Wu,G. (2007) Direct ^{23}Na NMR observation of mixed cations residing inside a G-quadruplex channel. *Chem. Commun.*, 795–797.
23. Ida,R. and Wu,G. (2008) Direct NMR detection of alkali metal ions bound to G-quadruplex DNA. *J. Am. Chem. Soc.*, **130**, 3590–3602.
24. Hud,N.V., Schultze,P. and Feigon,J. (1998) Ammonium ion as an NMR probe for monovalent cation coordination sites of DNA quadruplexes. *J. Am. Chem. Soc.*, **120**, 6403–6404.
25. Olson,C.M., Gmeiner,W.H. and Marky,L.A. (2006) Unfolding of G-quadruplexes: energetic, and ion and water contributions of G-quartet stacking. *J. Phys. Chem.*, **110**, 6962–6969.
26. Snoussi,K. and Halle,B. (2008) Internal sodium ions and water molecules in guanine quadruplexes: magnetic relaxation dispersion studies of $[d(G_3T_4G_3)]_2$ and $[d(G_4T_4G_4)]_2$. *Biochemistry*, **47**, 12219–12229.
27. Mergny,J.-L., De Cian,A., Ghelab,A., Saccà,B. and Lacroix,L. (2005) Kinetics of tetramolecular quadruplexes. *Nucleic Acids Res.*, **33**, 81–94.
28. Yan,Y.Y., Lin,J., Ou,T.-M., Tan,J.-H., Li,D., Gu,L.-Q. and Huang,Z.-S. (2010) Selective recognition of oncogene promoter G-quadruplexes by Mg^{2+}. *Biochem. Biophys. Res. Comm.*, **402**, 614–618.
29. Parkinson,G.N., Lee,M.P.H. and Neidle,S. (2002) Crystal structure of parallel quadruplexes from human telomeric DNA. *Nature*, **417**, 876–880.
30. Haider,S.M., Parkinson,G.N. and Neidle,S. (2003) Structure of a G-quadruplex-ligand complex. *J. Mol. Biol.*, **326**, 117–125.
31. Campbell,N.H., Patel,M., Tofa,A.B., Ghosh,R., Parkinson,G.N. and Neidle,S. (2009) Selectivity in ligand recognition of G-quadruplex loops. *Biochemistry*, **48**, 1675–1680.
32. Parkinson,G.N., Ghosh,R. and Neidle,S. (2007) Structural basis for binding of porphyrin to human telomeres. *Biochemistry*, **46**, 2390–2397.
33. Parkinson,G.N., Cuenca,F. and Neidle,S. (2008) Topology conservation and loop flexibility in quadruplex–drug recognition: crystal structures of inter- and intramolecular telomeric DNA quadruplex–drug complexes. *J. Mol. Biol.*, **381**, 1145–1156.
34. Campbell,N.H., Parkinson,G.N., Reszka,A.P. and Neidle,S. (2008) Structural basis of DNA quadruplex recognition by an acridine drug. *J. Am. Chem. Soc.*, **130**, 6722–6724.
35. Gray,R.D. and Chaires,J.B. (2011) Linkage of cation binding and folding in human telomeric quadruplex DNA. *Biophysical Chem.*, **159**, 205–209.
36. Wang,Y. and Patel,D.J. (1993) Solution structure of the human telomeric repeat d[AG3(T2AG3)3] G-tetraplex. *Structure*, **1**, 263–282.
37. Ambrus,A., Chen,D., Dai,J., Bialis,T., Jones,R.A. and Yang,D. (2006) Human telomeric sequence forms a hybrid-type intramolecular G-quadruplex structure with mixed parallel/antiparallel strands in potassium solution. *Nucleic Acids Res.*, **34**, 2723–2735.
38. Dai,J., Carver,M., Punchihewa,C., Jones,R.A. and Yang,D. (2007) Structure of the Hybrid-2 type intramolecular human telomeric G-quadruplex in K^+ solution: insights into structure polymorphism of the human telomeric sequence. *Nucleic Acids Res.*, **35**, 4927–4940.
39. Lim,K.W., Amrane,S., Bouaziz,S., Xu,W., Mu,Y., Patel,D.J., Luu,K.N. and Phan,A.T. (2009) Structure of the human telomere

in K$^+$ solution: a stable basket-type G-quadruplex with only two G-tetrad layers. *J. Am. Chem. Soc.*, **131**, 4301–4309.

40. Phan,A.T., Luu,K.N. and Patel,D.J. (2006) Different loop arrangements of intramolecular human telomeric (3+1) G-quadruplexes in K$^+$ solution. *Nucleic Acids Res.*, **34**, 5715–5719.

41. Luu,K.N., Phan,A.T., Kuryavyi,V., Lacroix,L. and Patel,D.J. (2006) Structure of the human telomere in K$^+$ solution: an intramolecular (3 + 1) G-quadruplex scaffold. *J. Am. Chem. Soc.*, **128**, 9963–9970.

42. Rankin,S., Reszka,A.P., Huppert,J., Zloh,M., Parkinson,G.N., Todd,A.K., Ladame,S., Balasubramanian,S. and Neidle,S. (2005) Putative DNA quadruplex formation within the human *c-kit* oncogene. *J. Am. Chem. Soc.*, **127**, 10584–10589.

43. Phan,A.T., Kuryavyi,V., Burge,S., Neidle,S. and Patel,D.J. (2007) Structure of an unprecedented G-quadruplex scaffold in the human *c-kit* promoter. *J. Am. Chem. Soc.*, **129**, 4386–4392.

44. Gunaratnam,M., Swank,S., Haider,S.M., Galesa,K., Reszka,A.P., Beltran,M., Cuenca,F., Fletcher,J.A. and Neidle,S. (2009) Targeting human gastrointestinal stromal tumor cells with a quadruplex-binding small molecule. *J. Med. Chem*, **52**, 3774–3783.

45. McLuckie,K.I., Waller,Z.A., Sanders,D.A., Alves,D., Rodriguez,R., Dash,J., McKenzie,G.J., Venkitaraman,A.R. and Balasubramanian,S. (2011) G-quadruplex-binding benzo[a]phenoxazines down-regulate c-KIT expression in human gastric carcinoma cells. *J. Am. Chem. Soc.*, **133**, 2658–2663.

46. Todd,A.K., Haider,S.M., Parkinson,G.N. and Neidle,S. (2007) Sequence occurrence and structural uniqueness of a G-quadruplex in the human *c-kit* promoter. *Nucleic Acids Res.*, **35**, 5799–5808.

47. Sheldrick,G.M. (2010) Experimental phasing with SHELXC/D/E: combining chain tracing with density modification. *Acta Crystallogr.*, **D66**, 479–485.

48. CCP4. (1994) The CCP4 suite: programs for protein crystallography. *Acta Crystallogr.*, **D50**, 760–763.

49. Emsley,P., Lohkamp,B., Scott,W.G. and Cowtan,K. (2010) Features and development of Coot. *Acta Crystallogr.*, **D66**, 486–501.

50. McCoy,A.J., Grosse-Kunstleve,R.W., Adams,P.D., Winn,M.D., Storoni,L.C. and Read,R.J. (2007) Phaser crystallographic software. *J. Appl. Crystallogr.*, **40**, 658–674.

51. Vagin,A.A., Steiner,R.A., Lebedev,A.A., Potterton,L., McNicholas,S., Long,F. and Murshudov,G.N. (2004) REFMAC5 dictionary: organization of prior chemical knowledge and guidelines for its use. *Acta Crystallogr.*, **D60**, 2184–2195.

52. Pettersen,E.F., Goddard,T.D., Huang,C.C., Couch,G.S., Greenblatt,D.M., Meng,E.C. and Ferrin,T.E. (2004) UCSF Chimera–a visualization system for exploratory research and analysis. *J. Comp. Chem*, **25**, 1605–1612.

53. DeLano,W.L. (2008) *The PyMOL Molecular Graphics System*, Version 0.99beta37, Schrödinger, LLC.

54. Woods,K.K., Maehigashi,T., Howerton,S.B., Sines,C.C., Tannenbaum,S. and Williams,L.D. (2004) High-resolution structure of an extended A-tract: [d(CGCAAATTTGCG)]$_2$. *J. Am. Chem. Soc.*, **126**, 15530–15531.

55. Cang,X., Sponer,J. and CheathamIII,T.E. (2011) Insight into G-DNA structural polymorphism and folding from sequence and loop connectivity through free energy analysis. *J. Am. Chem. Soc.*, **133**, 14270–14279.

56. Cang,X., Sponer,J. and CheathamIII,T.E. (2011) Explaining the varied glycosidic conformational, G-tract length and sequence preferences for anti-parallel G-quadruplexes. *Nucleic Acids Res.*, **39**, 4499–4512.

57. Reshetnikov,R.V., Sponer,J., Rassokhina,O.I., Kopylov,A.M., Tsvetkov,P.O., Makarov,A.A. and Govolin,A.V. (2011) Cation binding to 15-TBA quadruplex DNA is a multiple-pathway cation-dependent process. *Nucleic Acids Res.*, **39**, 9789–9802.